

Article

# Diverse Secondary Metabolites from the Marine-Derived Fungus *Dichotomomyces cejpai* F31-1

Yan-Xiu Chen <sup>1,2</sup>, Meng-Yang Xu <sup>1</sup>, Hou-Jin Li <sup>3</sup>, Kun-Jiao Zeng <sup>4</sup>, Wen-Zhe Ma <sup>5</sup>, Guo-Bao Tian <sup>4</sup>, Jun Xu <sup>1</sup>, De-Po Yang <sup>1,2</sup> and Wen-Jian Lan <sup>1,2,\*</sup>

<sup>1</sup> School of Pharmaceutical Sciences, Sun Yat-sen University, Guangzhou 510006, China; chenyx239@mail2.sysu.edu.cn (Y.-X.C.); xumy3@mail2.sysu.edu.cn (M.-Y.X.); junxu@biochemomes.com (J.X.); lssydp@mail.sysu.edu.cn (D.-P.Y.)

<sup>2</sup> Guangdong Technology Research Center for Advanced Chinese Medicine, Guangzhou 510006, China

<sup>3</sup> School of Chemistry, Sun Yat-sen University, Guangzhou 510275, China; ceslhj@mail.sysu.edu.cn

<sup>4</sup> Zhongshan School of Medicine, Sun Yat-sen University, Guangzhou 510080, China; zkj3880@163.com (K.-J.Z.); tiangb@mail.sysu.edu.cn (G.-B.T.)

<sup>5</sup> State Key Laboratory of Quality Research in Chinese Medicine, Macau Institute for Applied Research in Medicine and Health, Macau University of Science and Technology, Avenida Wai Long, Taipa 519020, Macau (SAR), China; wzma@must.edu.mo

\* Correspondence: lanwj@mail.sysu.edu.cn; Tel.: +86-20-3994-3042

Received: 30 August 2017; Accepted: 26 October 2017; Published: 1 November 2017

**Abstract:** By adding L-tryptophan and L-phenylalanine to GPY medium, twenty-eight compounds, including amides, polyketides, a sesquiterpenoid, a diterpenoid, a meroterpenoid, diketopiperazines,  $\beta$ -carboline, fumiquinazolines, and indole alkaloids, were discovered from the marine-derived fungus *Dichotomomyces cejpai* F31-1, demonstrating the tremendous biosynthetic potential of this fungal strain. Among these compounds, four amides dichotomocejs A–D (1–4), one polyketide dichocetide A (5), and two diketopiperazines dichocerazines A–B (15 and 16) are new. The structures of these new compounds were determined by interpreting detailed spectroscopic data as well as calculating optical rotation values and ECD spectra. Obviously, *Dichotomomyces cejpai* can effectively use an amino acid-directed strategy to enhance the production of nitrogen-containing compounds. Dichotomocej A (1) displayed moderate cytotoxicity against the human rhabdomyosarcoma cell line RD with an IC<sub>50</sub> value of 39.1  $\mu$ M, and pityriacitrin (22) showed moderate cytotoxicity against the human colon carcinoma cell line HCT116 with an IC<sub>50</sub> value of 35.1  $\mu$ M.

**Keywords:** *Dichotomomyces cejpai*; diverse secondary metabolites; amino acid-directed strategy; nitrogen-containing compounds; bioactivity

## 1. Introduction

The ascomycete *Dichotomomyces cejpai* is a common fungus known for its heat-resistant properties, that allow it to survive at 70 °C for 60 min [1]. *Dichotomomyces cejpai* is also representative of the fungus found in the soil under decomposing corpses, which highlights its potential as a forensic tool [2]. Extracts from this fungus display ciliostatic activity, cytotoxic activity, and broad-spectrum antimicrobial activity. In addition, *Dichotomomyces cejpai* has a substantial inhibitory effect on some drug-resistant bacterium [3–5]. The major metabolites of the fungus are diketopiperazines, indoloditerpenes, polyketides, and steroids. These secondary metabolites exhibited various bioactivities. For example, Henrik et al., isolated indoloditerpenes with antagonistic activities at GPR18 and cannabinoid receptors [6], one polyketide and three diketopiperazines with NF- $\kappa$ B inhibitory potentials [7], and one xanthocillin derivative and three steroids which can be  $\alpha$ -42 lowering agents [8]. In our effort to discover chemically diverse alkaloids of fungal origin with significant bioactivities, the metabolite

profile of the fungus *Dichotomomyces cejprii* F31-1 associated with the soft coral *Lobophytum crassum* collected in the South China Sea caught our attention. To encourage the fungus to generate alkaloids, we adopted the amino acid-directed strategy described previously [9,10]. By adding L-tryptophan and L-phenylalanine to GPY medium (20 g/L glucose, 5 g/L peptone, 2 g/L yeast extract, 30 g/L sea salt, and 1L H<sub>2</sub>O at pH 7.5), seven new compounds, including four aliphatic amides dichotomocejs A–D (1–4), one polyketide dichocetide A (5), and two diketopiperazines dichocerazines A–B (15 and 16), together with twenty-one known compounds (6–14, 17–28), were isolated from the EtOAc extract of the culture broth (Figure 1). The cytotoxicities of compounds 1, 7, 8, 11, 15, 22, 23, and 27 were evaluated against the four tumor cell lines HCT116, RD, ACHN, and A2780T, and the antimicrobial activities of compounds 4, 8, 13, 14, 22, and 24 were evaluated against the four bacteria ATCC29213, ATCC25922, ATCC27853, and ATCC19606. In this paper, we report the isolation, structural determination, and bioactivities of these compounds.

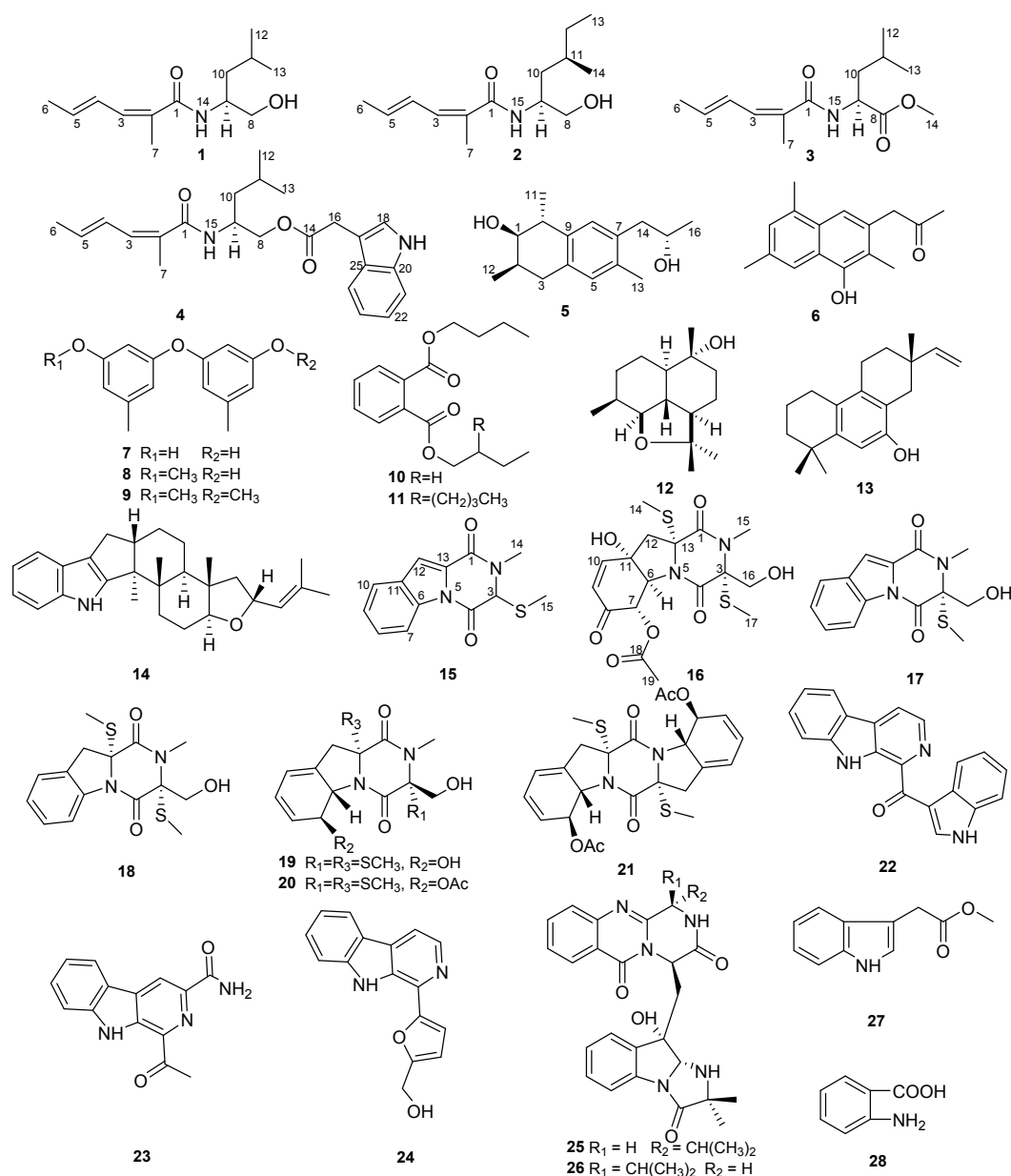
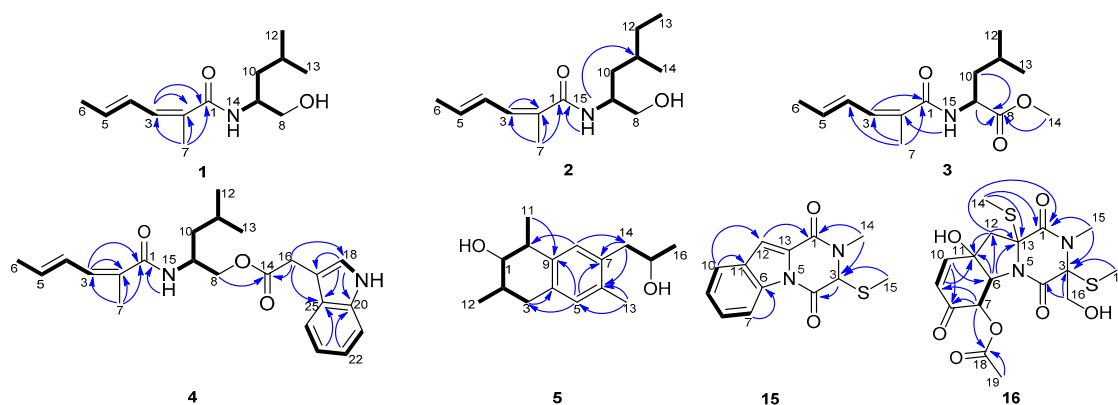


Figure 1. Chemical structures of compounds 1–28.

## 2. Results and Discussion

### 2.1. Structural Elucidation

Dichotomocej A (**1**) was afforded as a yellowish oil. The molecular formula was deduced to be  $C_{13}H_{23}NO_2$  from the HRESIMS quasi-molecular ion  $[M + H]^+$  peak at  $m/z$  226.1809 (calcd. for 226.1802) (Supplementary Figure S2), indicating three sites of unsaturation. The  $^{13}C$  NMR spectra (Table 1 and Supplementary Figure S4) showed thirteen carbons, including four methyls, two methylenes, two  $sp^3$  methines, three olefinic methines, one olefinic quaternary carbon, and one carbonyl. Therefore, the presence of two pairs of double bonds and one carbonyl accounts for the degrees of unsaturation. In addition, both the methine at  $\delta_C$  50.7 and the carbonyl at  $\delta_C$  170.4 were attached to a nitrogen atom, and the methylene at  $\delta_C$  67.1 was bonded to an oxygen atom. The  $^1H$  NMR data and HMQC spectra (Table 2 and Supplementary Figure S5) showed signals indicative of four methyl groups at  $\delta_H$  0.94 (d, 6.8), 0.95 (d, 6.8), 1.86 (d, 6.4), and 1.94 (s), two methylenes at  $\delta_H$  1.41 (dt, 8.4, 6.0) and 3.57 (dd, 10.8, 6.0)/3.72 (dd, 10.8, 3.2), two  $sp^3$  methines at  $\delta_H$  1.66 (m) and 4.12 (m), three olefinic methines at  $\delta_H$  6.04 (dq, 13.2, 6.8), 6.33 (ddq, 13.2, 11.2, 1.6), and 6.88 (d, 11.2), and one broad signal at  $\delta_H$  5.77 (brd, 6.4). The  $^1H$ - $^1H$  COSY correlations (Figure 2) of H-3 with H-4, H-4 with H-5, H-5 with H-6, and the key HMBC cross peaks (Figure 2) of H-7 with C-1/C-2/C-3 and H-3 with C-1/C-2 indicated the presence of a  $CH_3CH=CH-CH=C(CH_3)COX$  fragment. The  $^1H$ - $^1H$  COSY correlations of H-8 with H-9, H-9 with H-10, H-9 with H-14, H-10 with H-11, and H-11 with H-12/H-13 supported the right-hand aliphatic alcohol fragment of our proposed molecular structure. Thus, the structure of **1** was established as shown in Figure 1, which is similar to that of 2-methyl-hexa-2,4-dienoic acid, isoleucinol amide [11]. However the methylene of **1** at C-10 was not consistent with the aliphatic alcohol fragment present in the 2-methyl-hexa-2,4-dienoic acid, isoleucinol amide. Additionally in **1**, the geminal methyls at C-11 replaced a methyl and an ethyl fragment in the above mentioned analog. The double bond at C-4 of **1** was in the *E* configuration based on the large  $J_{H_4-H_5}$  coupling constant (13.2) and the NOESY correlation of H-3 with H-5. However, the double bond at C-2 was in the *Z* configuration based on the NOESY cross peaks of H<sub>3</sub>-7 with H-3/H-5. The absolute configuration of **1** was determined to be 9*S* based on the good match of the experimental optical rotation ( $-41.9$ ) with our calculated value ( $-42.1$ ) (Supplementary Table S1).



**Figure 2.** The  $^1H$ - $^1H$  COSY (bold line) and key HMBC correlations (arrows) of compounds **1**–**5** and **15**–**16**.

**Table 1.**  $^{13}C$  NMR data for compounds **1**–**5** and **15**–**16** (100 MHz,  $CDCl_3$ ).

No.	<b>1</b>	<b>2</b>	<b>3</b>	<b>4</b>	<b>5</b>	<b>15</b>	<b>16</b>
1	170.4, C	170.3, C	169.1, C	168.9, C	75.8, CH	156.7, C	165.8, C
2	127.3, C	127.2, C	127.3, C	127.3, C	31.0, CH	N	N
3	134.6, CH	134.6, CH	134.5, CH	134.1, CH	36.3, $CH_2$	66.8, CH	71.7, C
4	127.2, CH	127.1, CH	127.2, CH	127.1, CH	133.4, C	161.8, C	164.4, C

Table 1. Cont.

No.	1	2	3	4	5	15	16
5	136.7, CH	136.7, CH	136.6, CH	136.2, CH	130.5, CH	N	N
6	18.9, CH <sub>3</sub>	19.0, CH <sub>3</sub>	18.9, CH <sub>3</sub>	18.9, CH <sub>3</sub>	134.6, C	129.2, C	70.9, CH
7	13.0, CH <sub>3</sub>	13.0, CH <sub>3</sub>	12.9, CH <sub>3</sub>	12.6, CH <sub>3</sub>	134.4, C	116.5, CH	75.2, CH
8	67.1, CH <sub>2</sub>	66.4, CH <sub>2</sub>	174.0, C	66.6, CH <sub>2</sub>	130.6, CH	128.3, CH	190.9, C
9	50.7, CH	50.5, CH	51.1, CH	47.0, CH	138.6, C	125.7, CH	127.2, CH
10	40.5, CH <sub>2</sub>	38.3, CH <sub>2</sub>	42.1, CH <sub>2</sub>	40.8, CH <sub>2</sub>	37.8, CH	122.8, CH	148.4, CH
11	25.3, CH	31.5, CH	25.1, CH	24.9, CH	17.2, CH <sub>3</sub>	134.9, C	76.4, C
12	23.2, CH <sub>3</sub>	29.1, CH <sub>2</sub>	22.9, CH <sub>3</sub>	23.0, CH <sub>3</sub>	18.2, CH <sub>3</sub>	115.1, CH	51.1, CH <sub>2</sub>
13	22.4, CH <sub>3</sub>	11.2, CH <sub>3</sub>	22.3, CH <sub>3</sub>	22.4, CH <sub>3</sub>	19.3, CH <sub>3</sub>	127.9, C	69.4, C
14	NH	19.6, CH <sub>3</sub>	52.4, CH <sub>3</sub>	172.3, C	43.0, CH <sub>2</sub>	32.2, CH <sub>3</sub>	15.3, CH <sub>3</sub>
15		NH	NH	NH	68.1, CH	12.7, CH <sub>3</sub>	29.6, CH <sub>3</sub>
16				31.5, CH <sub>2</sub>	23.2, CH <sub>3</sub>		64.0, CH <sub>2</sub>
17				108.4, C			13.7, CH <sub>3</sub>
18				123.3, CH			170.1, C
19				NH			20.7, CH <sub>3</sub>
20				136.3, C			
21				111.5, CH			
22				122.3, CH			
23				119.8, CH			
24				118.8, CH			
25				127.4, C			

Table 2. <sup>1</sup>H NMR data for compounds 1–4 (400 MHz, CDCl<sub>3</sub>).

No.	1	2	3	4
3	6.88 (d, 11.2)	6.88 (d, 11.2)	6.88 (d, 10.8)	6.76 (d, 11.2)
4	6.33 (ddq, 13.2, 11.2, 1.6)	6.31 (ddq, 14.8, 11.2, 1.6)	6.32 (ddq, 15.2, 10.8, 1.6)	6.27 (ddq, 14.8, 11.2, 1.6)
5	6.04 (dq, 13.2, 6.8)	6.02 (dq, 14.8, 6.8)	6.03 (dq, 15.2, 6.8)	5.97 (dq, 14.8, 6.8)
6	1.86 (d, 6.4)	1.85 (d, 6.8)	1.85 (d, 6.4)	1.85 (d, 6.8)
7	1.94 (s)	1.93 (s)	1.95 (s)	1.72 (s)
8	3.57 (dd, 10.8, 6.0); 3.72 (dd, 10.8, 3.2)	3.55 (dd, 10.8, 6.0); 3.71 (dd, 10.8, 3.2)		4.09 (dd, 11.2, 4.0); 4.20 (dd, 11.2, 5.2)
9	4.12 (m)	4.11 (m)	4.71 (td, 8.4, 5.2)	4.33 (m)
10	1.41 (dt, 8.4, 6.0)	1.31 (dd, 13.2, 6.0); 1.54 (dt, 13.2, 6.4)	1.58 (m); 1.70 (m)	1.24 (m)
11	1.66 (m)	1.44 (m)	1.67 (m)	1.52 (m)
12	0.95 (d, 6.8)	1.14 (t, 6.8); 1.39 (m)	0.95 (d, 6.4)	0.85 (d, 6.4)
13	0.94 (d, 6.8)	0.86 (t, 6.8)	0.95 (d, 6.4)	0.85 (d, 6.4)
14	5.77 (brd, 6.4)	0.92 (d, 6.4)	3.74 (s)	
15		5.87 (brd, 7.2)	6.10 (d, 8.0)	5.54 (d, 8.8)
16				3.79 (s)
18				7.11 (s)
19				8.38 (brs)
21				7.34 (d, 8.0)
22				7.18 (dd, 8.0, 8.0)
23				7.11 (dd, 8.0, 8.0)
24				7.61 (d, 8.0)

Dichotomocej B (**2**) was obtained as a pale-yellow oil. This compound had a molecular formula of C<sub>14</sub>H<sub>25</sub>NO<sub>2</sub> based on the HRESIMS peak at *m/z* 240.1955 [M + H]<sup>+</sup> (calcd. for 240.1958) (Supplementary Figure S9) and had the same number of degrees of unsaturation as **1**. Careful inspection of the NMR

spectra (Tables 1 and 2, Supplementary Figures S10–S16) of **2** suggested that its NMR spectra resembled those of **1**. The only difference was a methyl and an ethyl fragment at C-11 in **2** instead of the geminal methyls seen in **1**. This was confirmed by the  $^1\text{H}$ - $^1\text{H}$  COSY cross peak (Figure 2) of H-12 with H-13 in **2**, and these substituents are consistent with the molecular formula of **2**. The double bond at C-4 of **2** was in the *E* configuration inferred by the large  $J_{\text{H4-H5}}$  coupling constant (14.8) and the NOESY correlation of H-3 with H-5, and the double bond at C-2 was in the *Z* configuration based on the NOESY correlations between H-3 and H-15 and between H<sub>3</sub>-7 and H-3/H-15.

The relative stereochemistry was inferred by the NOESY data. The NOESY correlations of H<sub>3</sub>-7 and H<sub>3</sub>-13 with H-9/H-11 revealed that H-9 and H-11 were located on the same side of the molecule. A comparison of the experimental optical rotation (−4.4) of **2** with the calculated value (−7.1) (Supplementary Table S1) suggested the stereochemistry of **2** was 9*S*, 11*R* since **2** only has two possible absolute configurations with opposite optical activities.

Dichotomocej C (**3**) was isolated as a yellowish oil. The HRESIMS spectrum of compound **3** gave a molecular ion peak at  $m/z$  254.1750  $[\text{M} + \text{H}]^+$  (calcd. for 254.1751) (Supplementary Figure S17), which suggested a molecular formula of  $\text{C}_{14}\text{H}_{23}\text{NO}_3$  with four degrees of unsaturation. The NMR data (Tables 1 and 2, Supplementary Figures S18–S24) of **3** were similar to those of **1**. The only significant difference was the presence of a methyl formate group at the C-8 position in **3** in place of the hydroxymethyl group seen in **1**. This finding was supported by the HMBC correlations (Figure 2) from H-9, H-10 and H-14 to C-8 and was consistent with the one additional degree of unsaturation in **3** relative to **1**. In addition, the configurations of the two double bonds in **3** were the same as those in **1**. This observation was based on the large  $J_{\text{H4-H5}}$  coupling constant (15.2) and the NOESY cross peaks of H-3 with H-5/H-15 and H<sub>3</sub>-7 with H-3/H-15. The experimental  $[\alpha]_{\text{D}}^{25}$  value (−51.6) of **3** showed the same direction of rotation as the calculated optical rotation (−48.4) (Supplementary Table S1), thus, **3** was assigned an absolute configuration of 9*S*.

Dichotomocej D (**4**) was afforded as a yellowish oil. Compound **4** showed a molecular ion peak at  $m/z$  383.2296  $[\text{M} + \text{H}]^+$  (calcd for 383.2329) in the HRESIMS spectrum (Supplementary Figure S25), which led us to give a molecular formula of  $\text{C}_{23}\text{H}_{30}\text{N}_2\text{O}_3$ , corresponding to ten double bond equivalents. The comparison of the NMR data (Tables 1 and 2, Supplementary Figures S26–S32) of **4** with those of **1** displayed that the alkyl chain of **4** was the same as that of **1**. The major difference was an indole acetoxyl in **4** replacing the hydroxyl group at C-8 in **1**, and the presence of that fragment accounts for the remaining degrees of unsaturation. The cross peaks of H-18 with H-19, H-21 with H-22, H-22 with H-23, and H-23 with H-24 in the  $^1\text{H}$ - $^1\text{H}$  COSY experiment (Figure 2) and the HMBC correlations (Figure 2) from H-8 to C-14, from H-16 to C-14/C-18/C-25, from H-18 to C-17/C-20/C-25, from H-22 to C-20, and from H-23 to C-25 further supported the indole acetoxyl group in **4**. Therefore, the proposed structure of **4** was shown in Figure 1. According to the large  $J_{\text{H4-H5}}$  coupling constant (14.8) and the NOESY cross peaks of H-3 with H-5/H-15 and H<sub>3</sub>-7 with H-3/H-15, the configurations of the double bonds in **4** were also identified as 2*Z*,4*E*. A calculated  $[\alpha]_{\text{D}}^{25}$  value (−14.5) of **4** was in consonance with the experimental value (−10.6) (Supplementary Table S1), indicating that the stereochemistry of **4** was 9*S*.

Dichocetide A (**5**) was isolated as a colorless oil and gave an HRESIMS ion peak at  $m/z$  271.16654  $[\text{M} + \text{Na}]^+$  (calcd. for 271.16685) (Supplementary Figure S33) that is indicative of the molecular formula of  $\text{C}_{16}\text{H}_{24}\text{O}_2\text{Na}$  with five sites of unsaturation. The  $^1\text{H}$ ,  $^{13}\text{C}$  NMR, DEPT and HMQC spectra (Tables 1 and 3, Supplementary Figures S34–S40) displayed signals for four methyls, two methylenes, six methines, and four quaternary carbons. Both C-1 and C-15 are connected to hydroxyl groups based on their downfield chemical shifts and the molecular formula of **5**. The  $\text{CH}_3\text{CHCH}(\text{OH})\text{CH}(\text{CH}_3)\text{CH}_2$  fragment was built from the  $^1\text{H}$ - $^1\text{H}$  COSY correlations (Figure 2) of H-2 with H-1/H-3/H-12 and of H-10 with H-1/H-11, and the  $\text{CH}_3\text{CH}(\text{OH})\text{CH}_2$  fragment was established based on the cross peaks of H-14 with H-15 and H-15 with H-16 in the  $^1\text{H}$ - $^1\text{H}$  COSY spectrum. Thorough analysis of the key HMBC cross peaks (Figure 2) from H-3 to C-4, from H-5 to C-3/C-7/C-9, from H-8 to C-10/C-14, from H-11 to C-9, from H-13 to C-5/C-6 and from H-14 to C-6/C-7 allowed us to connect the abovementioned

fragments. Thus, the planar structure of **5** was established as shown in Figure 1, and the partially reduced naphthalene ring core of **5** accounts for the five degrees of unsaturation.

The relative stereochemistry of **5** was confirmed by a NOESY experiment. The NOESY correlations of H-8 with H-10/H-15 suggested that H-10 and H-15 were located on the same side of the molecule as H-8. The experimental ECD spectrum (Figure 3) of **5** was identical to the curve calculated for (1*R*, 2*R*, 10*R*, 15*S*). Furthermore, the experimental optical rotation (23.0) is in accordance with the calculated value (25.1) (Supplementary Table S1), which supports the 1*R*, 2*R*, 10*R*, 15*S*-configuration of **5**.

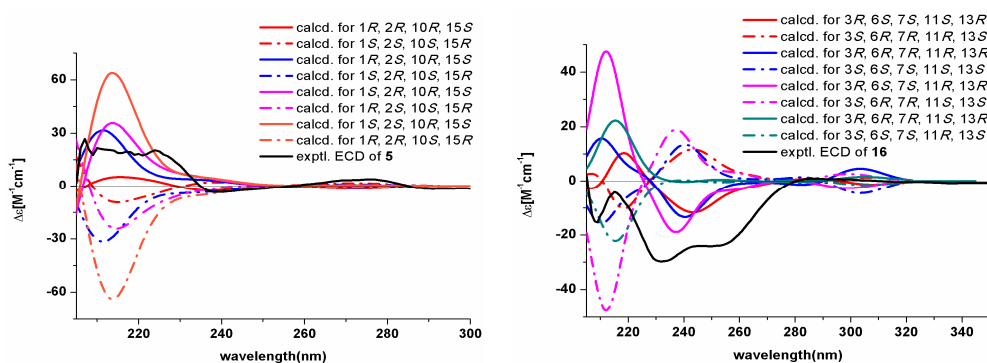


Figure 3. Comparison of the experimental and calculated ECD spectra of **5** and **16**.

Table 3. <sup>1</sup>H NMR data for compounds **5** and **15–16** (400MHz, CDCl<sub>3</sub>).

No.	<b>5</b>	<b>15</b>	<b>16</b>
1	3.71 (dd, 9.2, 4.8)		
2	2.07, m		
3	2.41 (dd, 16.8, 9.6); 2.92 (dd, 16.8, 6.4)	5.04 (s)	
5	6.87 (s)		
6			5.14 (d, 11.2)
7		8.42 (d, 8.0)	5.89 (d, 11.2)
8	6.94 (s)	7.53 (t, 8.0)	
9		7.40 (t, 8.0)	6.10 (d, 10.4)
10	3.03 (m)	7.70 (d, 8.0)	6.92 (d, 10.4)
11	1.25 (d, 7.2)		
12	1.11 (d, 6.4)	7.46 (s)	2.80 (d, 16.0); 3.42 (d, 16.0)
13	2.26 (s)		
14	2.67 (dd, 13.6, 8.4); 2.76 (dd, 13.6, 4.4)	3.24 (s)	2.23 (s)
15	4.00, m	2.05 (s)	3.10 (s)
16	1.27 (d, 6.4)		3.85 (d, 12.0); 4.31 (d, 12.0)
17			2.19 (s)
19			2.17 (s)

Dichocerazine A (**15**) was isolated as a yellowish solid. The molecular formula of compound **15** was determined to be C<sub>13</sub>H<sub>12</sub>N<sub>2</sub>O<sub>2</sub>S from the HRESIMS data, which showed a molecular ion peak at *m/z* 261.0686 [M + H]<sup>+</sup> (calcd. for 261.0692) (Supplementary Figure S59). This formula suggests nine degrees of unsaturation. The <sup>1</sup>H NMR spectrum (Table 3 and Supplementary Figure S60) displayed signals indicative of two singlet methyls at δ<sub>H</sub> 2.05 (s) and 3.24 (s), one sp<sup>3</sup> methine at δ<sub>H</sub> 5.04 (s), one aromatic proton at δ<sub>H</sub> 7.46 (s) and a 1,2-disubstituted benzene ring at δ<sub>H</sub> 7.40 (t, 8.0), 7.53 (t, 8.0), 7.70 (d, 8.0), and 8.42 (d, 8.0). The <sup>13</sup>C NMR, in combination with the DEPT experiment (Table 1 and Supplementary Figures S61 and S62) showed two methyls, six methines, and five quaternary carbons. Careful analysis of the 1D NMR data of **15** revealed characteristic signals of a diketopiperazine that were similar to the characteristic signals of 1,2,3,4-tetrahydro-2,3-dimethyl-1,4-dioxopyrazino[1,2-*a*]indole [12], except for an S-methyl at δ<sub>C</sub> 12.7 in **15** instead of the methyl at δ<sub>C</sub> 19.8 of the latter. Detailed 2D NMR analyses validated the planar structure of **15**, which was depicted in Figure 1. The HMBC

correlations (Figure 2) from H<sub>3</sub>-14 to C-1/C-3, from H-3 to C-4 and from H<sub>3</sub>-15 to C-3 supported the diketopiperazine framework. The <sup>1</sup>H-<sup>1</sup>H COSY correlations (Figure 2) of H-7 with H-8, H-8 with H-9 and H-9 with H-10 combined with the HMBC cross peaks of H-12 with C-1, H-10 with C-11/C-12 and H-7 with C-6 allowed us to determine the structure of the remaining fragments. Compound **15** didn't show optical activity in the optical rotation experiment, thus, this compound occurs as a racemate. The exhaustive effort to separate the enantiomers with HPLC using a Chiralcel OD column (250 mm × 10 mm) was unsuccessful.

Dichocerazine B (**16**) was acquired as a viscous yellow oil that gave an [M + Na]<sup>+</sup> ion in the HRESIMS at *m/z* 453.0727 (calcd. for 453.0761) (Supplementary Figure S67). Its molecular formula was determined to be C<sub>17</sub>H<sub>22</sub>N<sub>2</sub>O<sub>7</sub>S<sub>2</sub>, which implies eight double bond equivalents. From the NMR data (Tables 1 and 3, Supplementary Figures S68–S74), compound **16** was found to possess the same diketopiperazine skeleton as the 6-acetylbis (methylthio) gliotoxin previously isolated from *Neosartorya pseudofischeri* [12] based on the characteristic α-carbon signals of amino acid residues at δ<sub>C</sub> 69.4 and 71.7 and the two amide carbonyls at δ<sub>C</sub> 164.4 and 165.8. The presence of one *N*-methyl (δ<sub>C</sub> 29.6), one methylene connected to an oxygen atom (δ<sub>C</sub> 64.0), two *S*-methyls (δ<sub>C</sub> 13.7 and 15.3), and the cross peaks from H-14 to C-1/C-13, from H-15 to C-1/C-3, from H-16 to C-3/C-4, and from H-17 to C-3 in the HMBC spectrum verified the diketopiperazine fragment. Further inspection of the remaining data in the 1D NMR and HMQC experiments displayed one singlet methyl, one methylene, two sp<sup>2</sup> methines, two sp<sup>3</sup> methines attached to heteroatoms, one quaternary carbon linked to a heteroatom, one ester carbonyl, and one keto-carbonyl. Based on the <sup>1</sup>H-<sup>1</sup>H COSY correlations of H-9 with H-10 and H-6 with H-7, the two sp<sup>2</sup> methines were a pair of olefinic methines (δ<sub>C</sub> 127.2 and 148.4), and the two sp<sup>3</sup> methines were adjacent aliphatic methines (δ<sub>C</sub> 70.9 and 75.2). Detailed analyses of the HMBC correlations from H-6 to C-11/C-12/C-13, from H-12 to C-11/C-13, from H-7 to C-8/C-9/C-18, from H-9 to C-11, from H-10 to C-6/C-8, and from H-19 to C-18 confirmed the presence of a 6,5-fused ring system. In addition, the HMBC correlation of H-12 with C-1 explained the link between the diketopiperazine fragment and the 6,5-fused ring system. Consequently, the planar structure of **16** was constructed as shown in Figure 1.

The relative configuration of **16** was assigned by the magnitude of the coupling constant and the analysis of the NOESY spectrum (Supplementary Figure S74). The large *J*<sub>H-6/H-7</sub> (11.2) coupling constants suggested that both H-6 and H-7 are axial. The NOESY correlations of H-6 with H-12' and H-7 with H-12' indicated that H-6 and H-7 are trans to each other. Comparing the experimental CD curve and the [α]<sub>D</sub><sup>25</sup> value (−60.5) of **16** with the calculated ECD spectrum (Figure 3) and the optical rotation (−59.6) (Supplementary Table S1), respectively, the stereochemistry of **16** was confirmed to be 3*R*, 6*S*, 7*S*, 11*S*, 13*R*.

According to a comparison of the spectroscopic data of compounds **6–14** and **17–28** (Supplementary Figures S41–S58 and S75–S98) with literature reports, their chemical structures were identified as dichotone A (**6**) [13], diorcinol (**7**) [14], 3-*O*-methyl diorcinol (**8**) [14], 5,5'-oxybis(1-methoxy-3-methylbenzene) (**9**) [15], dibutyl phthalate (**10**) [16], butyl (2-ethylhexyl) phthalate (**11**) [17], (2*aR*, 5*R*, 5*aR*, 8*S*, 8*aS*)-2,2,5,8-tetramethyldecahydro-2*H*-naphtho[1,8-*bc*]furan-5-ol (**12**) [18], aspewentin A (**13**) [19], JBIR-03 (**14**) [20], dichotocepin A (**17**) [21], didehydrobisdethiobis (methylthio) gliotoxin (**18**) [12], bisdethiobis (methylthio) gliotoxin (**19**) [10], 6-acetylbis (methylthio) gliotoxin (**20**) [12], haematocin (**21**) [10], pityriacitrin (**22**) [22], stellarine A (**23**) [23], perlolyrine (**24**) [24], fiscalin C (**25**) [25], epi-fiscalin C (**26**) [25], indolyl-3-acetic acid methyl ester (**27**) [26], and anthranilic acid (**28**) [27].

## 2.2. Biological Activity

The cytotoxicities of compounds **1**, **7**, **8**, **11**, **15**, **22**, **23**, and **27** were evaluated against the human colon cancer cell line HCT116, human rhabdomyosarcoma cell line RD, human renal carcinoma cell line ACHN, and human ovarian cancer cell line A2780T. Dichotomocej A (**1**) exhibited a moderate inhibitory effect against RD with an IC<sub>50</sub> value of 39.1 μM, and pityriacitrin (**22**) exhibited a moderate inhibitory effect against HCT116 with an IC<sub>50</sub> value of 35.1 μM.

The antibacterial activities of compounds **4**, **8**, **13**, **14**, **22**, and **24** were screened against *Staphylococcus aureus* ATCC29213, *Escherichia coli* ATCC25922, *Pseudomonas aeruginosa* ATCC27853, and *Bauman's acinetobacter* ATCC19606. However, no significant inhibitory effects were observed for these compounds against these four bacterial strains.

### 3. Materials and Methods

#### 3.1. General Experimental Procedures

Column chromatography was carried out on silica gel (SiO<sub>2</sub>, 200–300 mesh, Qingdao Marine Chemical Inc., Qingdao, Shandong, China) and Sephadex LH-20 (green herbs, Beijing, China). Preparative HPLC was performed using a Shim-pack PRC-ODS HPLC column (250 × 20 mm, Shimadzu Corporation, Nakagyo-ku, Kyoto, Japan) and a Shimadzu LC-20AT HPLC pump (Shimadzu Corporation, Nakagyo-ku, Kyoto, Japan) installed with an SPD-20A dual λ absorbance detector (Shimadzu Corporation, Nakagyo-ku, Kyoto, Japan). 1D and 2D NMR spectra were measured on Bruker Avance II 400 spectrometers (Bruker BioSpin AG, Industriestrasse 26, Fällanden, Switzerland), and the chemical shifts are relative to the residual solvent signals (CDCl<sub>3</sub>: δ<sub>H</sub> 7.260 and δ<sub>C</sub> 77.160; Acetone-*d*<sub>6</sub>: δ<sub>H</sub> 2.050 and δ<sub>C</sub> 29.840; DMSO-*d*<sub>6</sub>: δ<sub>H</sub> 2.500 and δ<sub>C</sub> 39.520). Mass spectra were performed on Thermo DSQ ESI low-resolution and Thermo MAT95XP ESI high-resolution mass spectrometers (Thermo Fisher Scientific Inc., Waltham, MA, USA). UV spectra were acquired on a Shimadzu UV-Vis-NIR spectrophotometer (Shimadzu Corporation, Nakagyo-ku, Kyoto, Japan). IR spectra were recorded on a PerkinElmer Frontier FT-IR spectrophotometer (PerkinElmer Inc., Waltham, MA, USA). Optical rotations were recorded on a Schmidt and Haensch Polartronic HNQW5 optical rotation spectrometer (SCHMIDT + HAENSCH GmbH & Co., Berlin, Germany). CD spectra were obtained using a JASCO J-810 circular dichroism spectrometer (JASCO International Co. Ltd., Hachioji, Tokyo, Japan).

#### 3.2. Fungal Material

The marine fungus *Dichotomomyces cejpii* F31-1 was obtained from the inner tissue of the soft coral *Lobophytum crassum* collected from Hainan Sanya National Coral Reef Reserve, China. This fungal strain was conserved in 15% (*v/v*) glycerol aqueous solution at −80 °C. A voucher specimen was deposited in the School of Pharmaceutical Sciences, Sun Yat-sen University, Guangzhou, China. Analysis of the ITS rDNA (GenBank EF669956) by BLAST database screening provided a 100% match to *Dichotomomyces cejpii*.

#### 3.3. Culture, Extraction, and Isolation

The marine fungus *Dichotomomyces cejpii* was cultured in the medium which contained 20 g/L glucose, 5 g/L peptone, 2 g/L yeast extract, 2 g/L Trp, 2 g/L Phe, 30 g/L sea salt, and 1 L H<sub>2</sub>O at pH 7.5. Fungal mycelia were cut and transferred aseptically to 1 L Erlenmeyer flasks, each adding 600 mL of sterilized liquid medium. The flasks were incubated at 25 °C for 60 days. Ninety liters of liquid culture were filtered through cheesecloth to separate the culture broth and the mycelia. The culture broth was successively extracted three times with EtOAc (90 L) and then was concentrated by low-temperature rotary evaporation to give a crude extract (35 g).

The extract was chromatographed on a silica gel column (diameter: 8 cm, length: 80 cm, silica gel: 300 g) with a gradient of petroleum ether-EtOAc (10:0–0:10, *v/v*) followed by EtOAc-MeOH (10:0–0:10, *v/v*) to afford 12 fractions (Fr. 1–Fr. 12). Fr. 2 was purified by silica gel column using a step gradient elution with petroleum ether-EtOAc (10:0–0:10, *v/v*) to get 10 subfractions (Fr. 2-1–Fr. 2-10) after gathering the similar fractions as monitored by TLC analyses. Fr. 2-8 was separated via Sephadex LH-20 (MeOH) to give compounds **4** (17.2 mg), **8** (7.3 mg), and **22** (23.8 mg). Compounds **2** (2.0 mg) and **3** (3.5 mg) were obtained from Fr. 4 with a preparative RP HPLC with MeOH-H<sub>2</sub>O (61:39, *v/v*). Fr. 5 was purified by the recrystallization in the CHCl<sub>3</sub>-acetone (2:1, *v/v*) solution to afford compounds **23** (90.0 mg) and **24** (55.6 mg). Fr. 6 and Fr. 7 were subjected to a Sephadex LH-20 column and eluted with CH<sub>2</sub>Cl<sub>2</sub>-MeOH (1:1, *v/v*) to give three sub-fractions (Fr. 6-1–Fr. 6-3 and Fr.

7-1–Fr. 7-3) respectively. Then compounds **1** (7.2 mg), **13** (13.3 mg), **14** (0.6 mg), **15** (11.0 mg), and **27** (17.5 mg) were obtained from Fr. 6-2, which is chromatographed on silica gel column using a step gradient elution with  $\text{CHCl}_3$ -EtOAc (10:0–0:10, *v/v*). Fr. 7-1 was further purified with a preparative RP HPLC (MeCN- $\text{H}_2\text{O}$ , 35:65, *v/v*) to acquire compounds **11** (11.0 mg), **16** (7.6 mg), **5** (0.9 mg), and **26** (8.7 mg). Fr. 8 was recrystallized from MeOH to yield compound **18** (100.0 mg), while Fr. 9 was recrystallized from  $\text{CHCl}_3$  to produce compound **28** (32.0 mg). The mother liquid of Fr. 8 was further purified using reversed phase preparative HPLC with a mobile phase of MeOH- $\text{H}_2\text{O}$  (50:50, *v/v*) to obtain compounds **7** (70.8 mg), **19** (98.0 mg), **20** (110.2 mg), and **21** (6.8 mg). The mother liquid of Fr. 9 was isolated using Sephadex LH-20 (MeOH) to yield compounds **10** (27.5 mg) and **6** (1.8 mg). HPLC purification of Fr. 10 with solvent system MeCN- $\text{H}_2\text{O}$  (26:74, *v/v*) gave compounds **12** (10.2 mg) and **25** (4.5 mg). Finally, compounds **9** (6.9 mg) and **17** (7.0 mg) were separated by RP-HPLC with MeOH- $\text{H}_2\text{O}$  (66:34, *v/v*) of Fr. 10.

Dichotomocej A (**1**): pale yellow oil;  $[\alpha]_{\text{D}}^{25} = -41.9$  (*c* 0.30,  $\text{CHCl}_3$ ). UV (MeCN)  $\lambda_{\text{max}}$  nm (log  $\epsilon$ ): 192 (3.87), 253 (3.90). IR (KBr)  $\nu_{\text{max}}$  3367, 3233, 2957, 2926, 2870, 1652, 1629, 1530, 1378, 1262, 1050, 881  $\text{cm}^{-1}$ .  $^1\text{H}$  and  $^{13}\text{C}$  NMR data see Tables 1 and 2. HRESIMS  $m/z$  226.1809  $[\text{M} + \text{H}]^+$  (calcd. for  $\text{C}_{13}\text{H}_{23}\text{NO}_2$ , 226.1802).

Dichotomocej B (**2**): yellowish oil;  $[\alpha]_{\text{D}}^{25} = -4.4$  (*c* 0.20,  $\text{CHCl}_3$ ). UV (MeCN)  $\lambda_{\text{max}}$  nm (log  $\epsilon$ ): 193 (3.95), 245 (3.67). IR (KBr)  $\nu_{\text{max}}$  3377, 3223, 2959, 2926, 2855, 1652, 1529, 1378, 1261, 1051, 968, 804  $\text{cm}^{-1}$ .  $^1\text{H}$  and  $^{13}\text{C}$  NMR data see Tables 1 and 2. HRESIMS  $m/z$  240.1955  $[\text{M} + \text{H}]^+$  (calcd. for  $\text{C}_{14}\text{H}_{25}\text{NO}_2$ , 240.1958).

Dichotomocej C (**3**): yellowish oil;  $[\alpha]_{\text{D}}^{25} = -51.6$  (*c* 0.40,  $\text{CHCl}_3$ ). UV (MeCN)  $\lambda_{\text{max}}$  nm (log  $\epsilon$ ): 194 (4.35), 252 (4.05). IR (KBr)  $\nu_{\text{max}}$  3354, 2956, 2926, 2855, 1740, 1657, 1207, 1160  $\text{cm}^{-1}$ .  $^1\text{H}$  and  $^{13}\text{C}$  NMR data see Tables 1 and 2. HRESIMS  $m/z$  254.1750  $[\text{M} + \text{H}]^+$  (calcd. for  $\text{C}_{14}\text{H}_{23}\text{NO}_3$ , 254.1751).

Dichotomocej D (**4**): yellowish oil;  $[\alpha]_{\text{D}}^{25} = -10.6$  (*c* 0.20,  $\text{CHCl}_3$ ). UV (MeCN)  $\lambda_{\text{max}}$  nm (log  $\epsilon$ ): 192 (4.59), 220 (4.69), 257 (4.50). IR (KBr)  $\nu_{\text{max}}$  3389, 3233, 2957, 2926, 2870, 1727, 1633, 1514, 1457, 1260, 1157, 969, 737  $\text{cm}^{-1}$ .  $^1\text{H}$  and  $^{13}\text{C}$  NMR data see Tables 1 and 2. HRESIMS  $m/z$  383.2296  $[\text{M} + \text{H}]^+$  (calcd. for  $\text{C}_{23}\text{H}_{30}\text{N}_2\text{O}_3$ , 383.2329).

Dichocetide A (**5**): colorless oil;  $[\alpha]_{\text{D}}^{25} = 23.0$  (*c* 0.10, MeOH). CD (MeOH): 217 ( $\Delta\epsilon$  +21.4), 235 ( $\Delta\epsilon$  0), 239 ( $\Delta\epsilon$  -4.8), 257 ( $\Delta\epsilon$  0). UV (MeOH)  $\lambda_{\text{max}}$  nm (log  $\epsilon$ ): 202 (4.46), 270 (3.06), 280 (3.01). IR (KBr)  $\nu_{\text{max}}$  3201, 2970, 2926, 2907, 2857, 1739, 1376, 1263, 1051, 803  $\text{cm}^{-1}$ .  $^1\text{H}$  and  $^{13}\text{C}$  NMR data see Tables 1 and 3. HRESIMS  $m/z$  271.16654  $[\text{M} + \text{Na}]^+$  (calcd. for  $\text{C}_{16}\text{H}_{24}\text{O}_2\text{Na}$ , 271.16685).

( $\pm$ )-Dichocerazine A (**15**): yellowish solid;  $[\alpha]_{\text{D}}^{25} = 0$  (*c* 0.20, MeOH). UV (MeOH)  $\lambda_{\text{max}}$  nm (log  $\epsilon$ ): 202 (4.32), 245 (4.14), 272 (3.87), 298 (4.00). IR (KBr)  $\nu_{\text{max}}$  2926, 1712, 1651, 1588, 1569, 1429, 1385, 1359, 1333, 1256, 1207, 1019, 845, 749, 734  $\text{cm}^{-1}$ .  $^1\text{H}$  and  $^{13}\text{C}$  NMR data see Tables 1 and 3. HRESIMS  $m/z$  261.0686  $[\text{M} + \text{H}]^+$  (calcd. for  $\text{C}_{13}\text{H}_{12}\text{N}_2\text{O}_2\text{S}$ , 261.0692).

Dichocerazine B (**16**): viscous yellow oil;  $[\alpha]_{\text{D}}^{25} = -60.5$  (*c* 0.20, MeOH). CD (MeOH): 217 ( $\Delta\epsilon$  -4.6), 231 ( $\Delta\epsilon$  -29.8), 282 ( $\Delta\epsilon$  0). UV (MeOH)  $\lambda_{\text{max}}$  nm (log  $\epsilon$ ): 202 (4.21), 285 (3.39). IR (KBr)  $\nu_{\text{max}}$  3370, 2957, 2926, 2854, 1743, 1651, 1419, 1377, 1222, 1039  $\text{cm}^{-1}$ .  $^1\text{H}$  and  $^{13}\text{C}$  NMR data see Tables 1 and 3. HRESIMS  $m/z$  453.0727  $[\text{M} + \text{Na}]^+$  (calcd. for  $\text{C}_{17}\text{H}_{22}\text{N}_2\text{O}_7\text{S}_2$ , 453.0761).

### 3.4. Computational Methods

The absolute configurations of compounds **1–5** and **16** were determined by calculations of optical rotation values and ECD spectra. Both geometry analyses and all calculations of optical properties have been carried out using the Gaussian 09 software [28,29] and the theory of Boltzmann weights at room temperature. The stationary conformers with the lowest energy of compounds **1–5** and **16** were geometrically optimized by the DFT method at the B3LYP/6-31+G (d) level. The calculations of optical rotation values were performed by the TDDFT method at the B3LYP/6-31+G (d) level in

chloroform and methanol [29]. The ECD spectra of the different conformers were obtained using the TDDFT method at the PBE1PBE/6-311++G (d, p) level in methanol [30]. Additionally, the ECD spectra were generated from dipole-length dipolar and rotational strengths using a Gaussian band shape with a 0.3 eV exponential half-width and elaborated using the SpecDis program [31].

### 3.5. Cytotoxic Assay

The cytotoxic activities of the tested compounds against cancer cell lines were determined using sulforhodamine B (SRB) colorimetric method. Firstly, cells were seeded in 96 well plates in a volume of 100  $\mu\text{L}$ /well (5000–40,000 cells per well). After 24 h incubation at 37 °C in a humidified incubator with 5%  $\text{CO}_2$ , the cells were treated with 100  $\mu\text{L}$  medium containing tested compounds (2X indicated concentrations) for 72 h. Secondly, 50  $\mu\text{L}$  cold 50% (*w/v*) trichloroacetic acid (TCA) was applied to fix the attached cells for 1 h at 4 °C, and then 100  $\mu\text{L}$  0.4% (*w/v*) SRB was used for a stain of the attached cells. Finally, the protein-bound dye was solubilized with 200  $\mu\text{L}$  10 mM Tris base solution (pH 10.5) for absorbency determination at 515 nm by using SpectraMax 190 microplate reader (Molecular Devices). When the concentration was displayed as a 50% reduction in the process of cell growth, the  $\text{IC}_{50}$  value was defined.

### 3.6. Antimicrobial Activity

According to the National Committee for Clinical Laboratory Standards (NCCLS) standard, the antimicrobial experiments were performed using a broth dilution method (Mueller-Hinton broth). The tested bacteria were grown in liquid MH medium (2 g/L beef powder, 1.5 g/L soluble starch, 17.5 g/L acid hydrolyzed casein, PH = 7.4), and 50  $\mu\text{L}$  of bacterial suspension ( $1.5 \times 10^6$  CFU/mL) were seeded in 96 well plates. Then the test compounds (50  $\mu\text{L}$ ) with different concentrations were added into each well, 256  $\mu\text{g}/\text{mL}$  was a starting concentration to screen the potential antimicrobial activities of the tested compounds. The bacterial suspension without compounds was used as a positive control, while the MH medium was used as the negative control. After incubation at 37 °C in an electro-heating standing-temperature cultivator, the growth of the test organisms was inhibited completely with a lowest concentration. In this way, the minimum inhibitory concentration (MIC) of the tested compounds was defined. What's more, the OD determination at 595 nm were measured by a multifunction microplate reader (PowerWaveTMXS2, BioTek<sup>®</sup> Instruments Inc., Winooski, VT, USA).

## 4. Conclusions

In this study, twenty-eight compounds in total were obtained from the marine-derived fungus *Dichotomomyces cejpaii* F31-1. Their structures included amides, polyketides, a sesquiterpenoid, a diterpenoid, a meroterpenoid, diketopiperazines,  $\beta$ -carboline, fumiquinazolines and indole alkaloids, which demonstrated the tremendous biosynthetic potential of the investigated fungal strain. Seven diketopiperazines (15–21), four indole-related alkaloids (22–24, 27), and seven polyketides (5–11) had been previously reported from *Dichotomomyces cejpaii* in the literature, but four novel aliphatic amides (1–4) and two fumiquinazoline (25–26) alkaloids were also obtained. It was proposed that the fumiquinazolines are related to amino acids supplementation in the medium, since *Scedosporium apiospermum* F41-1 produced predominately fumiquinazolines when the medium was doped with exogenous amino acids [9]. Obviously, an amino acid-directed strategy is effective for promoting the production of nitrogen-containing compounds by *Dichotomomyces cejpaii*. Anthranilic acid, a common biosynthetic precursor of fumiquinazolines, was also isolated with the fumiquinazolines. Additionally, *Dichotomomyces cejpaii* also afforded indolyl-3-acetic acid methyl ester, which is apparently derived from tryptophan. Overall, the amino acids Trp and Phe in the culture medium of F31-1 may contribute to the generation and diversity of the nitrogen-containing compounds. Furthermore, the terpenoids (12 and 13) were the first of their chemical class reported from the genus *Dichotomomyces*.

**Supplementary Materials:** The following are available online at [www.mdpi.com/1660-3397/15/11/339/s1](http://www.mdpi.com/1660-3397/15/11/339/s1). Table S1: Comparison of the experimental optical rotation values with the calculated OR values of compounds 1–5 and 16; Figure S1: The most stable conformers of 1–5, 16; Figure S2: HR-ESI-MS spectrum of compound 1; Figure S3–S8: 1D and 2D NMR spectra of compound 1; Figure S9: HR-ESI-MS spectrum of compound 2; Figure S10–S16: 1D and 2D NMR spectra of compound 2; Figure S17: HR-ESI-MS spectrum of compound 3; Figure S18–S24: 1D and 2D NMR spectra of compound 3; Figure S25 HR-ESI-MS spectrum of compound 4; Figure S26–S32: 1D and 2D NMR spectra of compound 4; Figure S33: HR-ESI-MS spectrum of compound 5; Figure S34–S40: 1D and 2D NMR spectra of compound 5; Figures S41 and S42: 1D NMR spectra of compound 6; Figures S43 and S44: 1D NMR spectra of compound 7; Figures S45 and S46: 1D NMR spectra of compound 8; Figures S47 and S48: 1D NMR spectra of compound 9; Figures S49 and S50: 1D NMR spectra of compound 10; Figures S51 and S52: 1D NMR spectra of compound 11; Figures S53 and S54: 1D NMR spectra of compound 12; Figures S55 and S56: 1D NMR spectra of compound 13; Figures S57 and S58: 1D NMR spectra of compound 14; Figure S59: HR-ESI-MS spectrum of compound 15; Figures S60–S66: 1D and 2D NMR spectra of compound 15; Figure S67: HR-ESI-MS spectrum of compound 16; Figures S68–S74: 1D and 2D NMR spectra of compound 16; Figures S75 and S76: 1D NMR spectra of compound 17; Figures S77 and S78: 1D NMR spectra of compound 18; Figures S79 and S80: 1D NMR spectra of compound 19; Figures S81 and S82: 1D NMR spectra of compound 20; Figures S83 and S84: 1D NMR spectra of compound 21; Figures S85 and S86: 1D NMR spectra of compound 22; Figures S87 and S88: 1D NMR spectra of compound 23; Figures S89 and S90: 1D NMR spectra of compound 24; Figures S91 and S92: 1D NMR spectra of compound 25; Figures S93 and S94: 1D NMR spectra of compound 26; Figures S95 and S96: 1D NMR spectra of compound 27; Figures S97 and S98: 1D NMR spectra of compound 28.

**Acknowledgments:** This project is financially supported by the Guangdong Provincial Science and Technology Research Program (No. 2014A020217004, 2015A020216007, and 2016A020222004), the Guangzhou Science and Technology Research Program (No. 2014J4100059), and the Fundamental Research Funds for the Central Universities (No. 15ykpy05 and 14yksh01).

**Author Contributions:** Conceived of and designed the experiments: Wen-Jian Lan, Hou-Jin Li, De-Po Yang. Performed the experiments: Yan-Xiu Chen, Meng-Yang Xu, Kun-Jiao Zeng, Wen-Zhe Ma, Guo-Bao Tian. Wrote the paper: Yan-Xiu Chen, Wen-Jian Lan, Jun Xu.

**Conflicts of Interest:** The authors declare no conflict of interest.

## References

1. Jesenska, Z.; Pieckova, E.; Bernat, D. Heat-resitant fungi in the soil. *Int. J. Food Microbiol.* **1992**, *16*, 209–214. [[CrossRef](#)]
2. Tranchida, M.C.; Centeno, N.D.; Cabello, M.N. Soil fungi: Their potential use as a forensic tool. *J. Forensic Sci.* **2014**, *59*, 785–789. [[CrossRef](#)] [[PubMed](#)]
3. Pieckova, E.; Jesenska, Z. Toxinogenicity of heat-resistant fungi detected by a bio-assay. *Int. J. Food Microbiol.* **1997**, *36*, 227–229. [[CrossRef](#)]
4. Pieckova, E.; Roeijmans, H. Antibiotic secondary metabolites of *Dichotomomyces cejpuii*. *Mycopathologia* **1999**, *146*, 121–126. [[CrossRef](#)] [[PubMed](#)]
5. Rodrigues, B.S.; Sahm, B.D.; Jimenez, P.C.; Pinto, F.C.; Mafezoli, J.; Mattos, M.C.; Rodrigues-Filho, E.; Pfenning, L.H.; Abreu, L.M.; Costa-Lotufo, L.V.; et al. Bioprospection of cytotoxic compounds in fungal strains recovered from sediments of the brazilian coast. *Chem. Biodivers.* **2015**, *12*, 432–442. [[CrossRef](#)] [[PubMed](#)]
6. Harms, H.; Rempel, V.; Kehraus, S.; Kaiser, M.; Hufendiek, P.; Muller, C.E.; Konig, G.M. Indoloditerpenes from a marine-derived fungal strain of *Dichotomomyces cejpuii* with antagonistic activity at GPR18 and cannabinoid receptors. *J. Nat. Prod.* **2014**, *77*, 673–677. [[CrossRef](#)] [[PubMed](#)]
7. Harms, H.; Orlikova, B.; Ji, S.; Nesaei-Mosaferan, D.; Konig, G.M.; Diederich, M. Epipolythiodiketopiperazines from the marine derived fungus *Dichotomomyces cejpuii* with NF-kB inhibitory potential. *Mar. Drugs* **2015**, *13*, 4949–4966. [[CrossRef](#)] [[PubMed](#)]
8. Harms, H.; Kehraus, S.; Nesaei-Mosaferan, D.; Hufendieck, P.; Meijer, L.; Konig, G.M. Abeta-42 lowering agents from the marine-derived fungus *Dichotomomyces cejpuii*. *Steroids* **2015**, *104*, 182–188. [[CrossRef](#)] [[PubMed](#)]
9. Huang, L.H.; Xu, M.Y.; Li, H.J.; Li, J.Q.; Chen, Y.X.; Ma, W.Z.; Li, Y.P.; Xu, J.; Yang, D.P.; Lan, W.J. Amino acid-directed strategy for inducing the marine-derived fungus *Scedosporium apiospermum* F41-1 to maximize alkaloid diversity. *Org. Lett.* **2017**, *19*, 4888–4891. [[CrossRef](#)] [[PubMed](#)]

10. Lan, W.J.; Wang, K.T.; Xu, M.Y.; Zhang, J.J.; Lam, C.K.; Zhong, G.H.; Xu, J.; Yang, D.P.; Li, H.J.; Wang, L.Y. Secondary metabolites with chemical diversity from the marine-derived fungus *Pseudallescheria boydii* F19-1 and their cytotoxic activity. *RSC Adv.* **2016**, *6*, 76206–76213. [[CrossRef](#)]
11. Gallardo, G.L.; Butler, M.; Gallo, M.L.; Rodriguez, M.A.; Eberlin, M.N.; Cabrera, G.M. Antimicrobial metabolites produced by an intertidal *Acremonium furcatum*. *Phytochemistry* **2006**, *67*, 2403–2410. [[CrossRef](#)] [[PubMed](#)]
12. Liang, W.L.; Le, X.; Li, H.J.; Yang, X.L.; Chen, J.X.; Xu, J.; Liu, H.L.; Wang, L.Y.; Wang, K.T.; Hu, K.C.; et al. Exploring the chemodiversity and biological activities of the secondary metabolites from the marine fungus *Neosartorya pseudofischeri*. *Mar. Drugs* **2014**, *12*, 5657–5676. [[CrossRef](#)] [[PubMed](#)]
13. Huang, L.H.; Chen, Y.X.; Yu, J.C.; Yuan, J.; Li, H.J.; Ma, W.Z.; Watanapokasin, R.; Hu, K.C.; Niaz, S.; Yang, D.P.; et al. Secondary metabolites from the marine-derived fungus *Dichotomomyces* sp. L-8 and their cytotoxic activity. *Molecules* **2017**, *22*, 444. [[CrossRef](#)] [[PubMed](#)]
14. Wang, J.; Lu, Z.; Liu, P.; Wang, Y.; Li, J.; Hong, K.; Zhu, W. Cytotoxic polyphenols from the fungus *penicillium expansum* 091006 endogenous with the mangrove plant *excoecaria agallocha*. *Plant. Med.* **2012**, *78*, 1861–1866.
15. Sargent, M.V.; Stransky, P.O. Naturally occurring dibenzofurans. Part 1. A synthesis of cannabifuran. *J. Chem. Soc.* **1982**, 1605–1610. [[CrossRef](#)]
16. Li, J.T.; Yin, B.L.; Liu, Y.; Wang, L.Q.; Chen, Y.G. Mono-aromatic constituents of *Dendrobium longicornu*. *Chem. Natl. Compd.* **2009**, *45*, 234–236. [[CrossRef](#)]
17. Garba, S.; Salihu, L. Antibacterial activities of 2-o-butyl-1-o-(2'-ethylhexyl) benzene-1,8-dicarboxylate and 1-phenyl-1,4-pentanedione isolated from *Vitellaria paradoxa* root bark. *Asian J. Sci. Res.* **2011**, *4*, 149–157. [[CrossRef](#)]
18. Wu, L.S.; Hu, C.L.; Han, T.; Zheng, C.J.; Ma, X.Q.; Rahman, K.; Qin, L.P. Cytotoxic metabolites from *Perenniporia tephropora*, an endophytic fungus from *taxus chinensis* var. *Mairei*. *Appl. Microbiol. Biotechnol.* **2013**, *97*, 305–315. [[CrossRef](#)] [[PubMed](#)]
19. Miao, F.P.; Liang, X.R.; Liu, X.H.; Ji, N.Y. Aspewentins A–C, norditerpenes from a cryptic pathway in an algicolous strain of *Aspergillus wentii*. *J. Nat. Prod.* **2014**, *77*, 429–432. [[CrossRef](#)] [[PubMed](#)]
20. Ogata, M.; Ueda, J.Y.; Hoshi, M.; Hashimoto, J.; Nakashima, T.; Anzai, K.; Takagi, M.; Shinya, K. A novel indole-diterpenoid, JBIR-03 with anti-MRSA activity from *Dichotomomyces cejpui* var. *cejpui* NBRC 103559. *J. Antibiot.* **2007**, *60*, 645–648. [[CrossRef](#)] [[PubMed](#)]
21. Fan, Z.; Sun, Z.H.; Liu, Z.; Chen, Y.C.; Liu, H.X.; Li, H.H.; Zhang, W.M. Dichotocejpins A–C: New diketopiperazines from a deep-sea-derived fungus *Dichotomomyces cejpui* FS110. *Mar. Drugs* **2016**, *14*, 164. [[CrossRef](#)] [[PubMed](#)]
22. Mexia, N.; Gaitanis, G.; Velegraki, A.; Soshilov, A.; Denison, M.S.; Magiatis, P. Pityriazepin and other potent AhR ligands isolated from *malassezia furfur* yeast. *Arch. Biochem. Biophys.* **2015**, *571*, 16–20. [[CrossRef](#)] [[PubMed](#)]
23. Cui, Z.H.; Li, G.Y.; Qiao, L.; Gao, C.Y.; Wagner, H.; Lou, Z.C. Two new alkaloids from *stellaria dichotoma* var. *Lanceolata*. *Natl. Prod. Res.* **1995**, *7*, 59–64. [[CrossRef](#)]
24. Lee, S.H.; Jeong, S.J.; Jang, G.Y.; Kim, M.Y.; Hwang, I.G.; Kim, H.Y.; Woo, K.S.; Hwang, B.Y.; Song, J.; Lee, J.; et al. Isolation and identification of an antiproliferative compound from fructose-tryptophan maillard reaction products. *J. Agric. Food Chem.* **2016**, *64*, 3041–3047. [[CrossRef](#)] [[PubMed](#)]
25. Buttachon, S.; Chandrapatya, A.; Manoch, L.; Silva, A.; Gales, L.; Bruyère, C.; Kiss, R.; Kijjoa, A. Sartorymensin, a new indole alkaloid, and new analogues of tryptoquivaline and fiscalins produced by *Neosartorya siamensis* (KUFC 6349). *Tetrahedron* **2012**, *68*, 3253–3262. [[CrossRef](#)]
26. Nieman, J.; Coleman, J.; Wallace, D.; Piers, E.; Lim, L.; Roberge, M.; Andersen, R. Synthesis and antimitotic/cytotoxic activity of hemiasterlin analogues. *J. Nat. Prod.* **2003**, *66*, 183–199. [[CrossRef](#)] [[PubMed](#)]
27. Liang, W.W.; Wang, D.C.; Cheng, H.; Zhang, M.Z.; Zhang, Y.M.; Wei, D.S.; Qin, J.C. Chemical constituent from endophytic fungus *Chaetomium* sp. RSQMK-9 isolated from *Panax ginseng*. *Natl. Prod. Res. Dev.* **2014**, *26*, 1202–1206.
28. Frisch, M.J.; Trucks, G.W.; Schlegel, H.B.; Scuseria, G.E.; Robb, M.A.; Cheeseman, J.R.; Scalmani, G.; Barone, V.; Mennucci, B.; Petersson, G.A. *Gaussian 09*; Revision B.01; Gaussian: Pittsburgh, PA, USA, 2009.

29. Mazzeo, G.; Santoro, E.; Andolfi, A.; Cimmino, A.; Troselj, P.; Petrovic, A.G.; Superchi, S.; Evidente, A.; Berova, N. Absolute configurations of fungal and plant metabolites by chiroptical methods. Ord, ecd, and vcd studies on phyllostin, scytolide, and oxysporone. *J. Nat. Prod.* **2013**, *76*, 588–599. [[CrossRef](#)] [[PubMed](#)]
30. Pikulska, A.; Hopmann, K.H.; Bloino, J.; Pecul, M. Circular dichroism and optical rotation of lactamide and 2-aminopropanol in aqueous solution. *J. Phys. Chem. B* **2013**, *117*, 5136–5147. [[CrossRef](#)] [[PubMed](#)]
31. Polavarapu, P.L.; Scalmani, G.; Hawkins, E.K.; Rizzo, C.; Jeirath, N.; Ibnusaud, I.; Habel, D.; Nair, D.S.; Haleema, S. Importance of solvation in understanding the chiroptical spectra of natural products in solution phase: Garcinia acid dimethyl ester. *J. Nat. Prod.* **2011**, *74*, 321–328. [[CrossRef](#)] [[PubMed](#)]



© 2017 by the authors. Licensee MDPI, Basel, Switzerland. This article is an open access article distributed under the terms and conditions of the Creative Commons Attribution (CC BY) license (<http://creativecommons.org/licenses/by/4.0/>).